Available online at www.sciencedirect.com
SCIENCE DIRECT
Biochimica et Biophysica Acta 1758 (2006) 537–544
BIOCHIMICA ET BIOPHYSICA ACTA
BBA
http://www.elsevier.com/locate/bba

Pulling single bacteriorhodopsin out of a membrane: Comparison of simulation and experiment

Marek Cieplak [a,*], Sławomir Filipek [b], Harald Janovjak [c], Krystiana A. Krzyśko [b]

[a] Institute of Physics, Polish Academy of Sciences, Al. Lotników 32/46, 02-668 Warsaw, Poland
[b] International Institute of Molecular and Cell Biology, 02-109 Warsaw, Poland
[c] BioTechnological Center, University of Technology, 01307 Dresden, Germany

Received 14 January 2006; received in revised form 11 March 2006; accepted 14 March 2006
Available online 19 April 2006

Abstract

Mechanical unfolding of single bacteriorhodopsins from a membrane bilayer is studied using molecular dynamics simulations. The initial conformation of the lipid membrane is determined through all-atom simulations and then its coarse-grained representation is used in the studies of stretching. A Go-like model with a realistic contact map and with Lennard–Jones contact interactions is applied to model the protein–membrane system. The model qualitatively reproduces the experimentally observed differences between force-extension patterns obtained on bacteriorhodopsin at different temperatures and predicts a lack of symmetry in the choice of the terminus to pull by. It also illustrates the decisive role of the interactions of the protein with the membrane in determining the force pattern and thus the stability of transmembrane proteins.

Keywords: Mechanical stretching of protein; Go model; Molecular dynamic; Bacteriorhodopsin; Membrane; AFM

1. Introduction

Mechanical stretching of proteins by means of an atomic force microscope (AFM) is a valuable tool for the manipulation of single molecules that was especially well tested on the giant muscle molecule titin [1–5]. A common way to accomplish the stretching is to move the AFM tip by a displacement d at a constant velocity and monitor the force, F, that is generated by a protein anchored to a substrate. The interpretation of the F–d curves in terms of the unravelling events and properties of the protein requires theoretical modelling. Both all-atom [6–8] and coarse-grained [9–12] simulations have been employed to understand the unravelling of single domains of titin. The latter type of modelling was also used to understand stretching of multiple domains of titin [10–12] and of other proteins such as ubiquitin [13]. It should be noted that mechanical stretching of proteins is also a natural phenomenon that takes place in various cellular processes such as protein degradation by ATP-dependent proteases and, in particular, translocation through membranes [14–18]. Understanding the pulling and mechanical unfolding of bacteriorhodopsin (BR) out of a membrane can shed light on these processes.

One prediction coming from the simplified modelling on globular proteins [10,19] is that the force-displacement pattern depends on the temperature in a sensitive way because thermal fluctuations assist in unravelling. At lower temperatures, the peak forces are high and structured. At higher temperatures, the peak forces become weaker and occur earlier during the stretching. Finally, in the entropic limit [19], no individual force peaks can be identified and the F–d curve is described by the worm-like-chain model [20]. Furthermore, an increase in temperature results in a gradual transition from a serial, i.e., one-by-one, unravelling of multiple domains to a parallel, or simultaneous, unravelling. This means that the very sequencing of unfolding events depends on the choice of temperature.

The prediction of the sensitivity of the F–d pattern to temperature has found a qualitative confrmation in the recent studies of BR [21] and spectrin [22]. An example of the experimental results on BR is shown in Fig. 1 for the temperatures: 8, 25, and 52 °C. Unlike titin, however, BR is a membrane protein. Thus, the AFM pulling experiment results not only in stretching of the protein but also in extracting it out of the

* Corresponding author. Tel.: +48 22 843 6601x3365; fax: +48 22 843 0926.
E-mail address: mc@ifpan.edu.pl (M. Cieplak).

0005-2736/$ - see front matter © 2006 Elsevier B.V. All rights reserved.
doi:10.1016/j.bbamem.2006.03.028

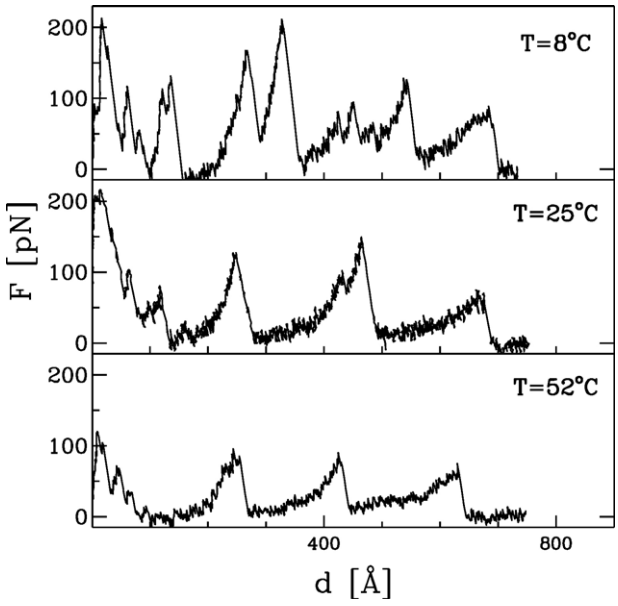

Fig. 1. Examples of the experimental force–displacement traces for bacteriorhodopsin being pulled out of a membrane by the C-terminus and for the temperatures indicated. The results are from reference [21] and they were obtained for the pulling velocity of 87 nm/s. Experimentally, pulling by the "C-terminus" means merely that the tip is attached near this terminus, not necessarily at the end point.

membrane. The force pattern then must depend on by which terminus the protein is pulled out and is influenced by interaction of the protein with the membrane.

In this paper, we provide a theoretical analysis of this system within a combined coarse-grained and all-atom approach. We show that this simplifed kind of modelling reproduces the experimental features in a qualitative manner and shows a distinct difference between pulling by the N- and C-termini. The C-terminus is located on the cytoplasmic side of the membrane. Currently, no experimental data on the N-terminal unfolding are available. Our modelling also shows the correct dependence on temperature. We provide insights into the stretching scenarios of bacteriodopsin and compare it to the stretching without a membrane. We show that the protein-membrane interactions dominate the *F–d* patterns. Our model adopts a simplifcation in which the membrane's conformation is held rigid during the pulling. Such a simplification is a natural step to adopt in what seems to be the first theoretical account of the protein–membrane stretching. It is expected that if the membrane was actually allowed to adjust dynamically to stretching by moving into the space just vacated by the protein, the dominance of the protein–membrane interaction in the *F–d* patterns would be enhanced even further than predicted here. The reason for this effect is that in an adjustable membrane the number the membrane–protein contacts does not significantly deplete for most of the stretching process.

There are many reasons to study the light-driven proton-pump BR. Its structural analysis has revealed the photoactive retinal embedded in seven closely packed transmembrane α-helices [23–27], a common structural motif among a large class of related G-protein coupled receptors [28–32]. Hydrophilic polypeptide loops link the seven membrane embedded hydrophobic BR helices lettered A, B, C, D, E, F and G, to which the C-terminus end is connected. The purple color of the chromophore and the proton-pumping activity of BR provide a direct measure of the correct folding of BR. As BR renatures efficiently from a denatured state into the functional protein [33] and with increasing knowledge of its structural and functional properties, it has become a paradigm for α-helical membrane proteins [34,35].

It was previously shown that single molecule AFM force measurements can be applied to unfold individual membrane proteins and determine the stability of their secondary structure elements [36–40]. In contrast to most forced unfolding experiments on globular proteins, membrane proteins unfold stepwise and thus these experiments yielded surprisingly detailed insights into inter- and intramolecular interactions [21,37,41]. In subsequent experiments, unfolding barriers stabilizing individual secondary structure elements of BR (such as transmembrane α-helices and polypeptide loops) were localized and the influence of external physiologically relevant parameters on these barriers was characterized [21,37].

2. Methods

We consider chain A of bacteriorhodopsin of Halobacterium salinarum the crystal structure of which has been determined [23] and given the 1BRR code in the Protein Data Bank [42]. It is an all-α protein. An alternative structure, 1AT9, of the same sequence (247 amino acids) has been determined by electron crystallography [43]. Another related sequence is that of halorhodopsin (HR), coded 1E12 (253 amino acids) [30]. We frst analyze stretching of the three structures in the absence of a membrane and show that they yield similar force patterns although 1E12 is more distinct, as expected. Then, we focus on 1BRR in studies that involve the membrane. It should be noted that stretching of BR and HR without a membrane can be accomplished only theoretically. The purpose of such simulations, however, is to ellucidate the role of the membrane.

To model the mechanical properties of the protein, we use the Go-like model [44,45] with the ground state corresponding to the conformation of the native state. This conformation is determined experimentally at room temperature. Our approach is outlined in references [10,46–49] and its first step is the determination of the native contacts between amino acids pair by pair and by checking for overlapping of the atoms in a way designed by Tsai et al. [50] and which is based on the van der Waals radii of the atoms (multiplied by a factor of 1.24 to account for the attractive part in the potential). There are 799 native contacts in 1BRR and they correspond to an average distance between the C^α atoms of 6.2 Å. The native contacts are described by the Lennard–Jones potentials:

$$V_{ij} = 4\varepsilon\left[\left(\frac{\sigma_{ij}}{r_{ij}}\right)^{12} - \left(\frac{\sigma_{ij}}{r_{ij}}\right)^{6}\right]. \quad (1)$$

The length parameters, σ_{ij}, in these potentials are selected so that the minima of the potentials agree with the experimentally determined distances between the C^α atoms at contact. The non-native contacts correspond to a repulsive core of σ=5 Å. The energy parameter, ϵ, is taken to be uniform and, when divided by the Boltzmann constant k_B, its value should be in the range 800–2300 K since it corresponds to an effective average of all non-covalent interactions in proteins. Our previous simulations of folding [10,49] were optimal with the dimensionless temperature $\tilde{T} = k_B T/\epsilon$ of order 0.3 which corresponds to room temperature if ϵ is around 900 K. Additionally, the simulated stretching curves were similar to experimental curves at $\tilde{T}$ =0.3 [10,11]. With ϵ=900 K, the unit of force used in this paper, ϵ/Å, corresponds to 120 pN. This choice also yields the correct magnitude of the force peak in titin [10] and ubiquitin [13] at room temperature. Therefore, 900 K should be considered to be a representative value of ϵ (see a further discussion of this point in reference [13]).

The tethering potential between the consecutive C^α atoms that binds them at the peptide bond length is purely harmonic with a strong spring constant of 100 ϵ/Å^2. The model also contains a four-body chirality term that favors the

native sense of chirality [51]. In our stretching simulations, both ends of the protein are attached to harmonic springs of elastic constant $k=0.12\ \epsilon/\text{Å}^2$ which is close to the values corresponding to the elasticity of experimental cantilevers. The free end of one of the two springs is constrained while the free end of the second spring is pulled at constant speed, v_p, along the initial end-to-end position vector. For proteins that are not buried in membranes and for quasistatic pulling the choice of the terminus to pull by is of no relevance. Otherwise, however, the force patterns are found to be distinct. We focus on v_p of 0.005 Å/τ, where $\tau=\sqrt{m\sigma 2}/\approx 3ps$ is the characteristic time for the Lennard–Jones potentials. Here, σ=5Å is a typical value of σ_{ij} and m is the average mass of the amino acids. The thermal fluctuations away from the native state are introduced by means of the Langevin noise, i.e., by random Gaussian forces together with a velocity dependent damping. This noise mimics the random effects of the solvent and, in particular, provides thermostating.

The temperature T controls structural fluctuations in the model protein including those which are present under room temperature even though the ground state of our model corresponds to the native state of the protein that was determined at room temperature. In order to account for a finite resolution within which the thermal effects are observed to affect the force–displacement relationship, we average the forces over a pulling distance of 0.5 Å.

An equation of motion for each C^α reads

$$m\ddot{r} = -\gamma\dot{r} + F_c + \Gamma. \quad (2)$$

F_c is the net force due to the molecular potentials and Γ is the random force of the Gaussian character. The damping constant γ is taken to be equal to 2 m/τ and the dispersion of the random forces is equal to $\sqrt{2\gamma k_B T}$. This choice of γ corresponds to a situation in which the inertial effects are negligible [49] but the damping action is not yet as strong as in water. Increasing γ tenfold results in a tenfold increase in the time scales (see, e.g., Ref. [52] bringing the typical value of v_p within two orders of magnitude of the experimental pulling speeds [10,49]. The equations of motion are solved by a fifth order predictor–corrector scheme.

In order to study the coupled protein–membrane system, we immerse the 1BRR structure into an all-atom model of a lipid bilayer. Both layers are considered as being made of the POPC (1-palmitoyl-2-oleoyl-*sn*-glycero-3-phosphatidylcholine) phospholipids. Molecular dynamics simulations were performed by using Yasara program (v.5.1 Yasara Biosciences) with Amber99 force feld [53]. The parameters for POPC and coordinates of equilibrated POPC membrane fragment were taken from [54,55]. The long-range electrostatic interactions were treated by the PME (Particle Mesh Ewald) algorithm [56]. After minimizing the energy, molecular dynamics calculations were performed in a periodic box flled with 5020 molecules of water, as modelled with the TIP3P potential, under the atmospheric pressure and temperature of 300 K. During the frst 100 ps of equilibration, the protein and the membrane were frozen and water with sodium and chloride counterions were allowed to move. After this stage, the membrane was thawed and the system was equilibrated for another 300 ps. The water molecules that were still residing in cavities between phospholipids were then removed manually. At this stage, a 1-ns molecular dynamics simulation was applied to all molecules in the system, including the protein. The size of the periodicity box was made to shrink in the 1-ns stage of the simulations to assure the best ft between the membrane and the protein and to remove empty regions from the membrane hydrophobic part. The fnal box dimensions within the plane of the membrane were 6.5×6.5 nm and the plane consisted of 106 POPC molecules. The box length in the perpendicular direction was equal to 8.5 nm. Each side of the membrane patch was formed by

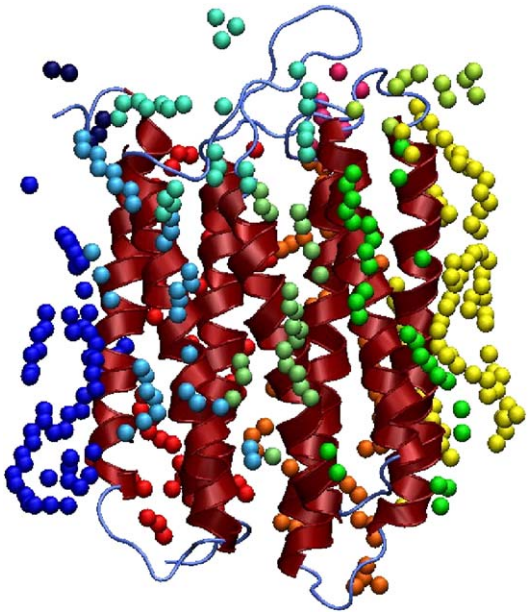

Fig. 3. The bacteriorhodopsin–membrane system in the coarse-grained representation of the membrane: only those carbon atoms are shown which make contact with bacteriorhodopsin 1BRR in its native state. The average C^α–C distance in such contacts is close to the average C^α–C^α contact distance in the protein. The terminus shown at the top of the figure is of the N-type and the one at the bottom of the C-type. The colors assigned to the phospholipids indicate the identity of the closest helix of BR. The color convention used is as in Fig. 2.

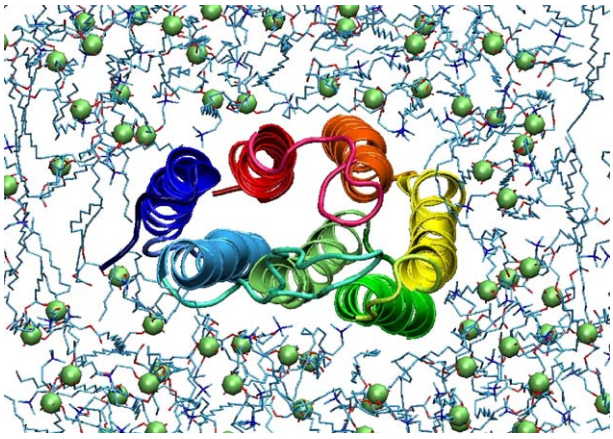

Fig. 2. The bacteriorhodopsin-membrane system at the end of the all-atom simulations. The helices of BR are colored from blue (helix 1) to red (helix 7). The protein is represented by the helices. In the membrane subsystem, the green spheres indicate locations of the phosphorus atoms. The remaining parts of the lipids are shown schematically.

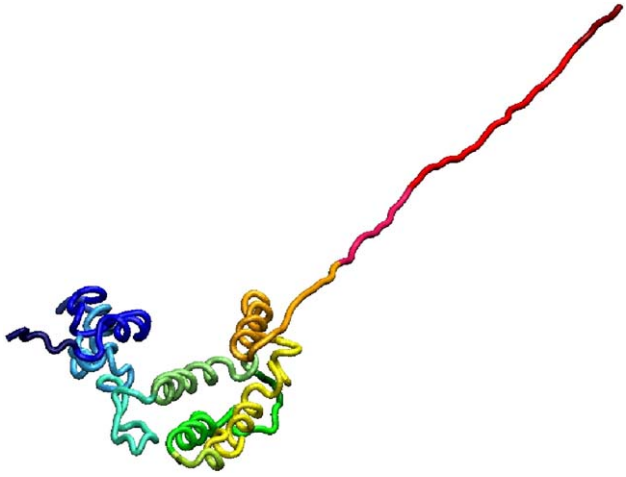

Fig. 4. Example of the backbone conformation of the model bacteriorhodopsin when stretched by the terminus C. The molecules of the membrane are not shown.

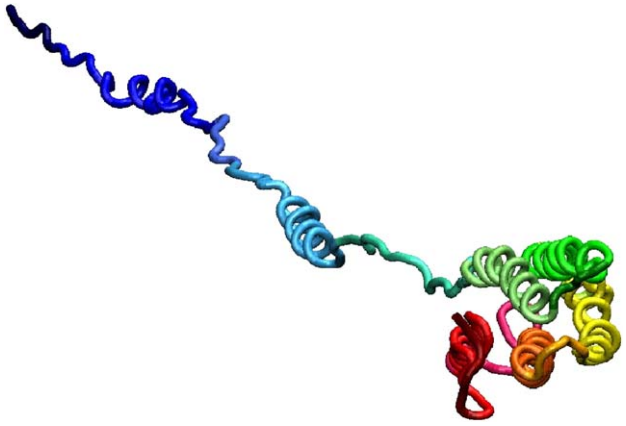

Fig. 5. Example of the backbone conformation of the model bacteriorhodopsin when stretched by the terminus N. The molecules of the membrane are not shown.

approximately 8 phospholipid molecules. The resulting conformation of the system is shown in Fig. 2. This conformation is the starting state in the studies of stretching.

We adopt an approximation in which the membrane is held frozen during the stretching. Furthermore, in order to provide a unifed coarse grained description of the whole system, we represent the membrane merely by all of its carbon atoms. In a chemistry-based simulation, it would be important to also include atoms of phosphorus and oxygen. However, in a purely geometry based-modelling, it is sufficient to render the geometry by considering just the carbon atoms. We determine which of these carbon atoms form contacts in the starting conformation by using the overlap based procedure of Tsai et al. [50] again (with the van der Waals radius of the atomic group C4H1 through C4H3 of 1.88 Å). There are 359 carbon atoms which make 495 contacts with the protein and these atoms, together with the bacteriorhodopsin are shown in Fig. 3 in a sideway projection. The Lennard–Jones potentials are assigned to these contacts. For simplicity, the strength of the protein–membrane couplings is taken to be equal to ϵ the strength of the contacts within the protein. The snapshots of the backbone of the protein stretched by termini C and N are shown in Figs. 4 and 5 respectively. Both fgures correspond to a simulational displacement of 200 Å and they are clearly distinct.

It should be pointed out that the Go-like description of the system has certain unphysical features which relate to the fact that the native structure is heavily favored energetically. Thus, when a helix is moved along the membrane, the system is penalized, in the model, by the departure from the native conformation, whereas, in fact, it may fnd itself happy in a new local minimum of the energy. Similarly, shearing motions within the protein need not be necessarily energetically costly. Further work is required to deal with such modelling limitations.

It is interesting to note that another version of the Go model for a protein–membrane system has been proposed by Orlandini et al. [57] to investigate folding kinetics of a two-helix fragment of BR. The membrane was represented by a slab of width 26 Å so that the native protein contacts acquire a lower energy when within the slab to enhance its stability there. The non-atomic structure of the model makes it unsuitable, however, to study stretching since most of the related dynamical effects take place inside the membrane.

3. Results and discussion

We first consider stretching of BR and HR without any surrounding lipid molecules. Fig. 6 shows examples of stretching curves for bacteriorhodopsin and three values of the reduced temperature. The curves do depend on the temperature in a manner discussed in general in references [10,19]. The higher the temperature, the lower the peak forces because thermal fluctuations assist in unfolding. It is interesting to note that the values of the peak forces are similar to those obtained for the I27 domain of titin (made of only 89 amino acids) within the same model [10,11]. However, the peaks are much wider and the traces are overall quite distinct. When one compares traces obtained for two available structures for the same sequence, 1BRR and 1AT9, one can see that the traces can be distinguished when no thermal fuctuations are present (the top panel of Fig. 6). However, at $\tilde{T}=0.3$ which usually appears to play the role of the room temperature, the two patterns are hard to distinguish (the one for 1AT9 is not shown for visual clarity). Fig. 7 shows that HR 1E12 has peak forces similar to those of bacteriorhodopsin but the patterns are different than those shown in Fig. 6. It should be noted that all these patterns show similarities in the initial stages of stretching—for d less than about 200 Å. Another similarity lies in the qualitative dependence on the temperature.

We now consider the bacteriorhodopsin system with the membrane. Figs. 8 and 9 show the force–displacement curves when the protein is pulled by the C- and N-termini respectively. At each temperature studied, they are clearly distinct. The maximal force in our simulations is by a factor of two higher than for the I27 domain of titin within a similar Go-like model (and no membrane). (Experimentally, the maximal force in I27 is of order 200 pN [3,4] and the maximal force in the BR–membrane system is comparable.) It is also substantially higher compared to the system without a membrane, indicating that the dynamics are dominated by breaking of the protein–membrane contacts. The discrepancy between the theoretical predictions and experimental fndings on the absolute values of the maximal forces when compared to titin may have two sources: (a) the effective value of for BR might be lower than the one that appears to work for titin (about 900 K), (b) it is possible that the effective interactions with the membrane are smaller (maybe by the factor of two) than those within the protein. This effect may be produced by entropic factors introduced by the membrane. Despite the uncertainty in

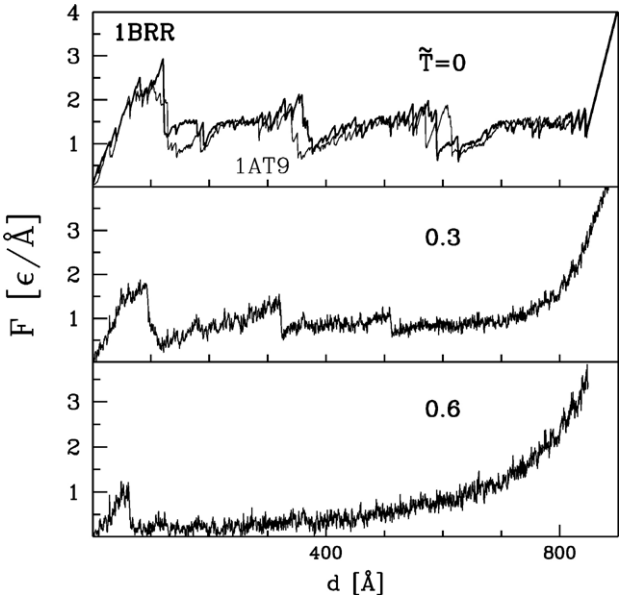

Fig. 6. Theoretical force–displacement relationships for two structures corresponding to bacteriorhodopsin at the reduced temperatures as indicated. The thick solid lines are for 1BRR, whereas the thin line (only in the top panel) is for 1AT9.

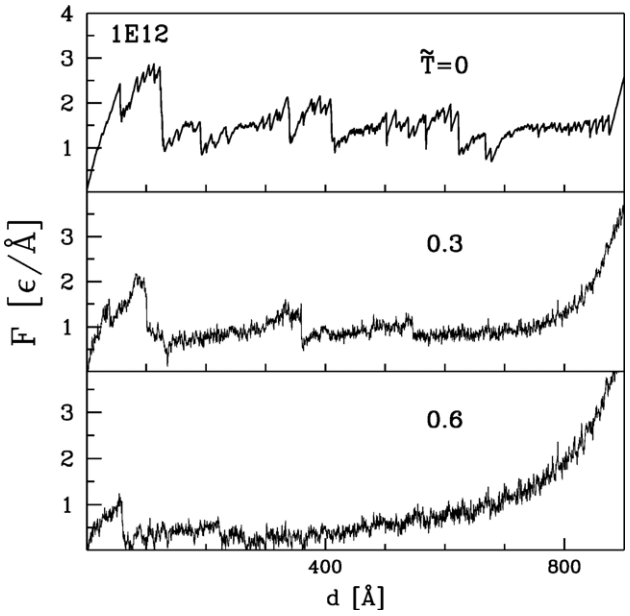

Fig. 7. Theoretical force–displacement relationships for halorhodopsin at the reduced temperatures as indicated.

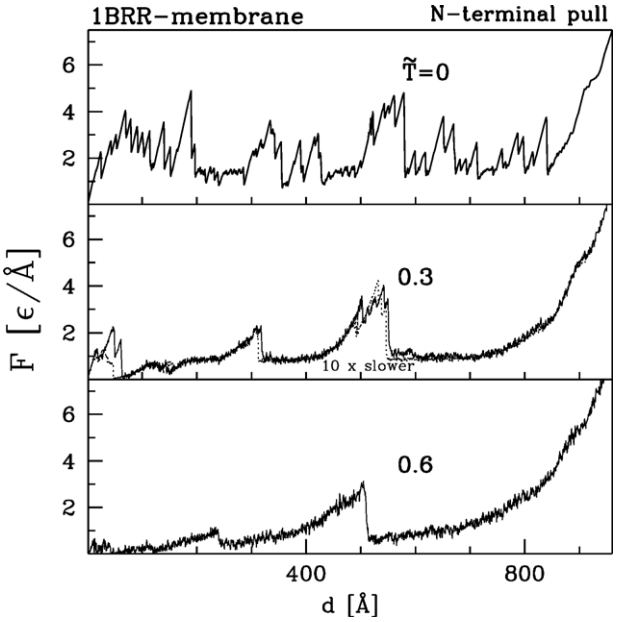

Fig. 9. Theoretical force–displacement relationships for bacteriorhodopsin corresponding to structure 1BRR as it is being pulled out of the membrane by the terminus N. The thin line in the middle panel corresponds to $v_p = 0.0005$ Å/τ.

the theoretical value of the magnitude of the peak forces, the force–displacement pattern itself shows a remarkable similarity to the one observed experimentally. This is illustrated in Fig. 10 which compares the room temperature trace to the rescaled theoretical trace at $\tilde{T}=0.3$. The rescaling affects the value of ϵ/σ–its effective value is taken to be of order 30 pN– and of d. The rescaling factor for the displacement, Υ, is taken to be 1.35. The fact that Υ is larger than 1 refects the fact that the experimental cantilever stiffness is smaller than used in the simulations. We have found [9] that the smaller the stiffness, the longer the displacement at which a given peak force arises. The similarity of the traces extends throughout the whole process of pulling except within the frst 10 nm. In this region at the beginning, the experimental data are affected by the apparatus effects in which the dynamics are affected by non-specifc electrostatic interactions between the AFM tip and the membrane surfaces.

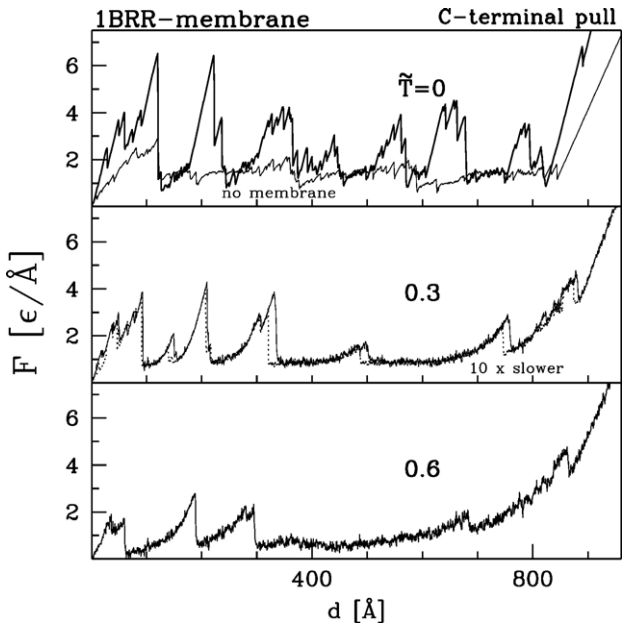

Fig. 8. Theoretical force–displacement relationships for bacteriorhodopsin corresponding to structure 1BRR as it is being pulled out of the membrane by the terminus C. The thin line in the top panel shows the $\tilde{T}=0$ result without the membrane (a repeat of the thick line in the top panel of Fig. 6). The thin line in the middle panel corresponds to $v_p = 0.0005$ Å/τ.

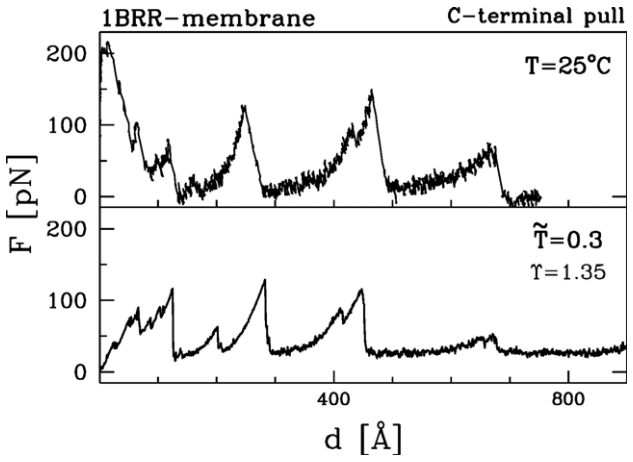

Fig. 10. Comparison of the experimental (top) and theoretical (bottom) force–displacement traces. The theoretical values of F and d were rescaled as explained in the text. In the experiment, every single molecule shows a characteristic force pattern such as the one shown here. In every trace, three main peaks are observed above the distance of 150 Å. Occasionally, they split into up to three peaks each, indicating that the unfolding process involves single helices rather than helical pairs [37]. The simulation is capable of clearly resolving peaks at distances below 150 Å which is hard to do experimentally since the short displacements are dominated by strong unspecific tip–surface interactions.

When assessing the infuence of the choice of the pulling terminus, we note that the pull by the C-terminus at $\tilde{T}=0.3$ results in three groups of strong peaks within the frst 400 Å of the process. On the other hand, the N-terminal pull results in only two groups and is characterized by forces weaker by the factor of two. At the highest temperature studied, of 0.6, the N-terminal pull yields essentially no peaks within the frst 400 Å and one major peak around 550 Å. In contrast, there are three major peaks for the C-terminal pull and they are all found within the frst 300 Å. It should be noted that the peaks within the frst 400 Å of the C-terminal stretching are of particular interest because they correspond to unfolding of the helices that are associated with the functionality of the retinal pigment. However, in the experiments, this region is infuenced by non-specifc surface interactions between the membrane and the AFM tip.

The middle panels of Figs. 8 and 9 compare the patterns generated at the pulling speed of 0.005 Å/τ (the thicker lines) to those obtained at a speed which is an order of magnitude slower. We observe that there are merely some minor logarithmic shifts that relate to the choice of v_p. This is consistent with the experimentally established logarithmic dependence of peak height on pulling rate for proteins that are stretched without a membrane [3,58–60].

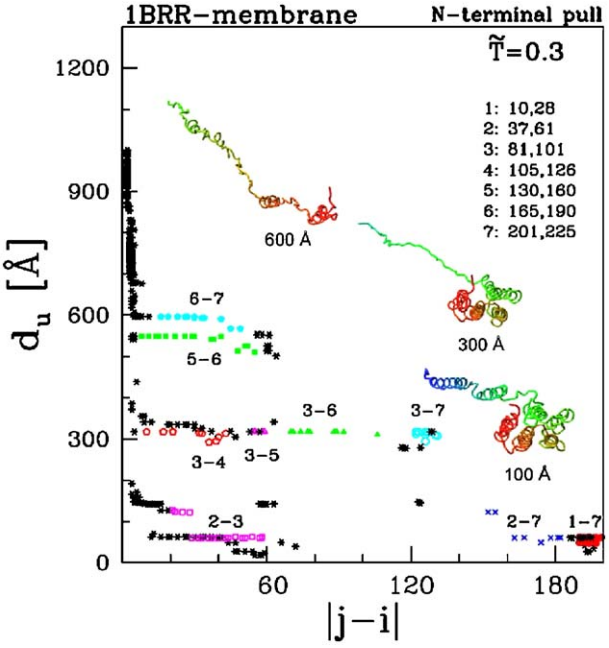

Fig. 12. Same as in Fig. 10 but for pulling by the N-terminus.

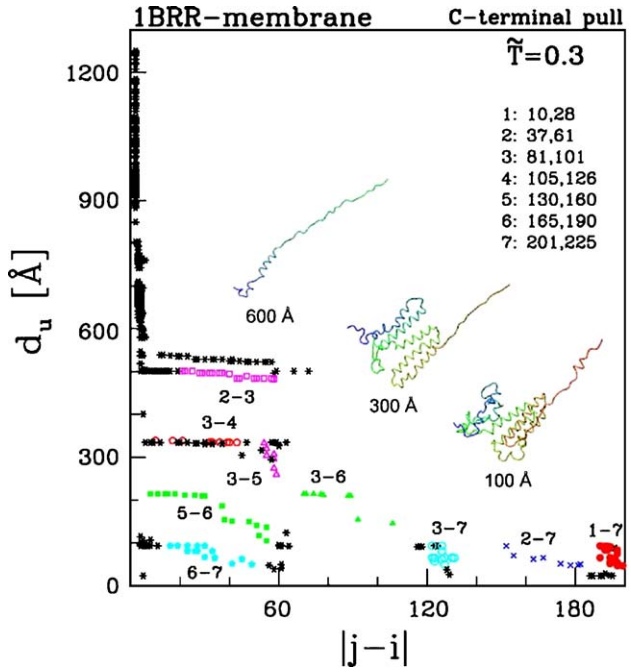

Fig. 11. The $\tilde{T}=0.3$ stretching scenarios of bacteriorhodopsin corresponding to pulling by the C-terminus. The scenario is defined in terms of last tip displacements, d_u, at which specific native contacts still hold. The contacts between amino acids i and j are first identified by the sequential distance, $|j-i|$, between them. The more detailed identification is provided by labels, such as 1–7, which specify contacts between specific helices. There are seven helices which correspond to the sequential locations listed on the top right of the figure. For instance, helical segment 1 corresponds to amino acids between with the sequential locations between 10 and 28, segment 2—between 37 and 61, etc. Thus, contacts denoted as 1–7 are those which are made between helix 1 (amino acids between 10 and 28) and helix 7 (locations between 201 and 225). The symbols (different shapes and different colors) indicate particular types of contacts, such as 1–7. In addition to plotting the values of d_u, the Figure also shows snapshots of bacteriorhodopsin at an extension d written at the bottom of each snapshot.

Finally, we discuss the predicted order in which the contacts in the protein are ruptured when the protein is being pulled out of the membrane. We investigate the average tip displacement distance, d_u, at which these contacts break definitely as a function of the contact order. The contact order is defned as the sequential distance, $|j-i|$, between a pair of amino acids i and j that make a contact in the native state. For a contact to hold we require that the C^α–C^α distance does not exceed $1.5\sigma_{ij}$. Figs. 11

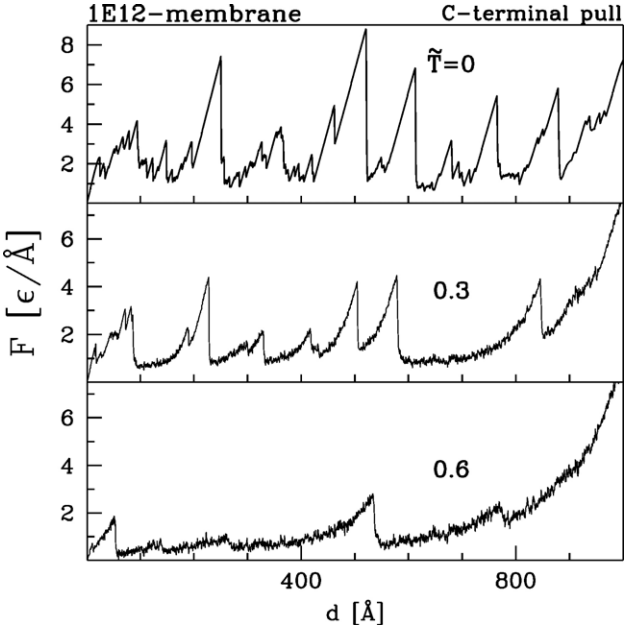

Fig. 13. Theoretical force–displacement relationships for halorhodopsin corresponding to structure 1E12 as it is being pulled out of the membrane by the terminus C at the temperatures indicated.

and 12 show the rupture distances d_u at $\tilde{T}=0.3$ for the C- and N-terminal pull respectively. The peak forces can be identifed in these diagrams by accumulation of points along horizontal stretches because such an accumulation corresponds to a nearly simultaneous rapture of many contacts. It is seen that even though the two ways of pulling start in a similar way (by breaking the contacts between sequencial regions 2 and 7 as well as between 1 and 7, as defned in Figs. 11 and 12) the differences between the two ways of pulling arise early. The main difference is in the order in which the contacts denoted by 2–3 break relative to the contacts denoted by 5–3; essentially, they switch. When the N-terminus is pulled, the 2–3 contacts rupture very early and the 5–3 contacts break late. It is the other way around when the C-terminus is pulled. There is also a similar, but less dramatic, switch between the order of breaking of the 3–4 and 5–6 interhelical contacts.

A recent experimental study by Cisneros et al. [40] suggested that BR and halorohodopsin show similar but not identical unfolding patterns. Results of our simulations of HR with the membrane are summarized in Fig. 13. They indicate an even stronger dependence on temperature than in the case of BR. For instance, the force peaks at $\tilde{T}=0$ on Fig. 13 are higher than in Fig. 8. At the same time, a much smaller number of peaks persists at $\tilde{T}=0.6$. The middle panel, corresponding to $\tilde{T}=0.3$–the analog of the room temperature situation–shows that up the frst 300 Å in the displacement, the force patterns for BR and HR are alike but beyond this distance they diverge.

The simulated *F–d* traces for BR with the membrane for the C-terminal pulling show features which are similar to the experimental ones, especially when it comes to the dependence on temperature. It should be noted that there is a varying offset of the experimental curves due to picking up a random amino acid near the C-terminus. In both the simulation and the experiment, three groups of peaks are found which have approximately the same relative heights. Remarkably, the N-terminal pulling curves look very different from the simulated and experimental C-terminal curves. Only two groups of peaks are predicted for the N-terminal case. This indicates that the unfolding pattern of a membrane protein is directional. In contrast to our simplifed simulations which involve a single monomeric BR, the experimental unfolding curves were collected on trimeric BR. However, the striking similarities between simulation and experiment indicate that the measured force pattern is an intrinsic property of the (monomeric) structure of the protein. This prediction is also experimentally supported by an on-going study by Sapra et al. [61].

As already found for the *F–d* curves, there are also clear similarities in the unfolding sequence of the simulation and the experiment. The experiments have reported step-wise unfolding of BR helix by helix from 7 to 1 [37]. This seems to be reproduced in the simulations since the contacts that unravel frst involve helices 6 and 7, which happens for d_u below 200 Å. This is then followed by a loss in contacts of helix 5 between 200 and 300 Å. In agreement with the experiment, helix 4 then unfolds in a distinct group of peaks at d_u of approximately 320 Å. In a last step, and again in qualitative agreement with the experiment, the next group of peaks at $d_u=500$ Å corresponds to unfolding of helices 2 and 3.

We conclude that a simple coarse grained Go-like model captures the essential features of the experimental results obtained on the bacteriorhodopsin–membrane system and predicts a major lack of symmetry between the two choices of the terminus to pull by.

Acknowledgements

This work was funded by the Ministry of Science and Informatics in Poland (grants 2P03B 03225 and 3P05F 02625). The modelling was partly done at the ICM Computer Centre, Warsaw University, Poland. HJ was supported by the European Union and the Free State of Saxony (grant to D. J. Mueller).

References

[1] H.P. Erickson, Stretching single protein molecules: titin is a weird spring, Science 276 (1997) 1090.
[2] M.S.Z. Kellermayer, S.B. Smith, H.L. Granzier, C. Bustamante, Folding–unfolding in single titin molecules characterized with laser tweezers, Science 276 (1997) 1112–1116.
[3] M. Rief, M. Gautel, F. Oesterhelt, J.M. Fernandez, H.E. Gaub, Reversible unfolding of individual titin immunoglobulin domains by AFM, Science 276 (1997) 1109–1112.
[4] M. Carrion-Vasquez, A.F. Oberhauser, S.B. Fowler, P.E. Marszalek, S.E. Broedel, J. Clarke, J.M. Fernandez, Mechanical and chemical unfolding of a single protein: a comparison, Proc. Natl. Acad. Sci. U. S. A. 96 (1999) 3694–3699.
[5] A.F. Oberhauser, P.E. Marszalek, M. Carrion-Vazquez, J.M. Fernandez, Single protein misfolding events captured by atomic force microscopy, Nat. Struct. Biol. 6 (1999) 1025–1028.
[6] H. Lu, B. Isralewitz, A. Krammer, V. Vogel, K. Schulten, Unfolding of titin immunoglobulin domains by steered molecular dynamics simulation, Biophys. J. 75 (1998) 662–671.
[7] H. Lu, K. Schulten, Steered molecular dynamics simulation of conformational changes of immunoglobulin domain I27 interpreted atomic force microscopy observations, Chem. Phys. 247 (1999) 141–153.
[8] E. Paci, M. Karplus, Unfolding proteins by external forces and temperature: the importance of topology and energetics, Proc. Natl. Acad. Sci. U. S. A. 97 (2000) 6521–6526.
[9] M. Cieplak, T.X. Hoang, M.O. Robbins, Folding and stretching in a Go-like model of titin, Proteins: Struct. Funct. Biol. 49 (2002) 114–124.
[10] M. Cieplak, T.X. Hoang, M.O. Robbins, Thermal effects in stretching of Go-like models of titin and secondary structures, Proteins: Struct. Funct. Biol. 56 (2004) 285–297.
[11] M. Cieplak, A. Pastore, T.X. Hoang, Mechanical properties of the domains of titin in a Go-like model, J. Chem. Phys. 122 (2004) 054906.
[12] M. Cieplak, Mechanical stretching of proteins: calmodulin and titin, Physica, A 352 (2004) 28–42.
[13] M. Cieplak, P.E. Marszalek, Mechanical unfolding of ubiquitin molecules, J. Chem. Phys. 123 (2005) 194903.
[14] S. Huang, K.S. Ratliff, A. Matouschek, Protein unfolding by the mitochondrial membrane potential, Nat. Struct. Biol. 9 (2002) 301–307.
[15] S. Prakash, A. Matouschek, Protein unfolding in the cell, Trends Biochem. Sci. 29 (2004) 593–600.
[16] R.J. Deshaies, S.L. Sanders, D.A. Feldheim, R. Schekman, Assembly of yeast Sec proteins involved in translocation into the endoplasmic reticulum into a membrane-bound multisubunit complex, Nature 349 (1991) 806–808.
[17] G. Schatz, B. Dobberstein, Common principles of protein translocation across membranes, Science 271 (1996) 1519–1526.
[18] R.E. Dalbey, M. Chen, Sec-translocase mediated membrane protein biogenesis, Biochim. Biophys. Acta 1694 (2004) 37–53.
[19] M. Cieplak, T.X. Hoang, M.O. Robbins, Stretching of proteins in the entropic limit, Phys. Rev., E Stat. Nonlin. Soft Matter Phys. 69 (2004) 011912.

[20] M. Doi, S.F. Edwards, Theory of Polymer Dynamics, Oxford University Press, Oxford, 1988.
[21] H. Janovjak, M. Kessler, D. Oesterhelt, H.E. Gaub, D.J. Mueller, Unfolding pathways of native bacteriorhodopsin depend on temperature, EMBO J. 22 (2003) 5220–5229.
[22] R. Law, G. Liao, et al., Pathway shifts and thermal softening in temperature-coupled forced unfolding of spectrin domains, Biophys. J. 85 (2003) 3286–3293.
[23] L.-O. Essen, R. Siegert, W.D. Lehmann, D. Oesterhelt, Lipid patches in membrane protein oligomers: crystal structure of the bacteriorhodopsin–lipid complex, Proc. Natl. Acad. Sci. U. S. A. 95 (1998) 11673–11678.
[24] K. Mitsuoka, T. Hirai, et al., The structure of bacteriorhodopsin at 3.0 Å resolution based on electron crystallography: implication of the charge distribution, J. Mol. Biol. 286 (1999) 861–882.
[25] H. Belrhali, P. Nollert, A. Royant, C. Menzel, J.P. Rosenbusch, E.M. Landau, E. Pebay-Peyroula, Protein, lipid and water organization in bacteriorhodopsin crystals: a molecular view of the purple membrane at 1.9 Å resolution, Struct. Fold. Des. 7 (1999) 909–917.
[26] N. Grigorieff, T.A. Ceska, K.H. Downing, J.M. Baldwin, R. Henderson, Electron-crystallographic refnement of the structure of bacteriorhodopsin, J. Mol. Biol. 259 (1996) 393–421.
[27] H. Luecke, B. Schobert, H.T. Richter, J.P. Cartailler, J.K. Lanyi, Structure of bacteriorhodopsin at 1.55 Å resolution, J. Mol. Biol. 291 (1999) 899–911.
[28] J.M. Baldwin, The probable arrangement of the helices in G protein-coupled receptors, EMBO J. 12 (1993) 1693–1703.
[29] E.J.M. Helmreich, K.P. Hofmann, Structure and function of proteins in G-protein-coupled signal transfer, Biochim. Biophys. Acta 1286 (1996) 285–322.
[30] M. Kolbe, H. Besir, L.-O. Essen, D. Oesterhelt, Structure of the light-driven chloride pump halorhodopsin at 1.8 Å resolution, Science 288 (2000) 1390–1396.
[31] K. Palczewski, T. Kumasaka, T. Hori, C.A. Behnke, H. Motoshima, B.A. Fox, I. Le Trong, D.C. Teller, T. Okada, R.E. Stenkamp, et al., Crystal structure of rhodopsin: a G-protein coupled receptor, Science 289 (2000) 739–745.
[32] A. Royant, P. Nollert, K. Edman, R. Netze, E.M. Landau, E. Pebay-Peyrouts, J. Navarro, X-ray structure of sensory rhodopsin II at 2.1 Å resolution, Proc. Natl. Acad. Sci. U. S. A. 98 (2001) 10131–10136.
[33] K.S. Huang, H. Bayley, et al., Refolding of an integral membrane protein. Denaturation, renaturation, and reconstitution of intact bacteriorhodopsin and two proteolytic fragments, J. Biol. Chem. 256 (1981) 3802–3809.
[34] J.K. Lanyi, Progress toward an explicit mechanistic model for the light-driven pump, bacteriorhodopsin, FEBS Lett. 464 (1999) 103–107.
[35] S. Subramanian, The structure of bacteriorhodopsin: an emerging consensus, Curr. Opin. Struct. Biol. 9 (1999) 462–468.
[36] C. Moeller, D. Fotiadis, et al., Determining molecular forces that stabilize human aquaporin-1, J. Struct. Biol. 142 (2003) 369–378.
[37] D.J. Mueller, M. Kessler, F. Oesterhelt, C. Moeller, D. Oesterhelt, H.E. Gaub, Stability of bacteriorhodopsin alpha-helices and loops analyzed by single-molecule force spectroscopy, Biophys. J. 83 (2002) 3578–3588.
[38] F. Oesterhelt, D. Oesterhelt, M. Pfeiffer, A. Engel, H.E. Gaub, D.J. Mueller, Unfolding pathways of individual bacteriorhodopsins, Science 288 (2000) 143–146.
[39] A. Kedrov, C. Ziegler, et al., Controlled unfolding and refolding of a single sodium-proton antiporter using atomic force microscopy, J. Mol. Biol. 340 (2004) 1143–1152.
[40] D.A. Cisneros, D. Oesterhelt, et al., Probing origins of molecular interactions stabilizing the membrane proteins halorhodopsin and bacteriorhodopsin, Structure 13 (2005) 235–242.
[41] H. Janovjak, J. Struckmeier, M. Hubain, A. Kedrov, M. Kessler, D.J. Mueller, Probing the energy landscape of the membrane protein bacteriorhodopsin, Structure 12 (2004) 871–879.
[42] F.C. Bernstein, T.F. Koetzle, G.J.B. Williams, E.F. Meyer Jr., M.D. Brice, J. R. Rodgers, O. Kennard, T. Shimanouchi, M. Tasumi, The Protein Data Bank: a computer-based archival file for macromolecular structures, J. Mol. Biol. 112 (1977) 535–542.
[43] Y. Kimura, D.G. Vassylyev, A. Miyazawa, A. Kidera, M. Matsushima, K. Mitsuoka, K. Murata, T. Hirai, Y. Fujiyoshi, Surface of bacteriorhodopsin revealed by high-resolution electron crystallography, Nature 389 (1997) 206–211.
[44] H. Abe, N. Go, Noninteracting local-structure model of folding and unfolding transition in globular proteins II. Application to two-dimensional lattice proteins, Biopolymers 20 (1981) 1013–1031.
[45] S. Takada, Going for the prediction of protein folding mechanism, Proc. Natl. Acad. Sci. U. S. A. 96 (1999) 11698–11700.
[46] T.X. Hoang, M. Cieplak, M. Molecular dynamics of folding of secondary structures in Go-like models of proteins, J. Chem. Phys. 112 (2000) 6851–6862.
[47] T.X. Hoang, M. Cieplak, Sequencing of folding events in Go-like proteins, J. Chem. Phys. 113 (2001) 8319–8328.
[48] M. Cieplak, T.X. Hoang, Kinetics non-optimality and vibrational stability of proteins, Proteins: Struct. Funct. Biol. 44 (2001) 20–25.
[49] M. Cieplak, T.X. Hoang, Universality classes in folding times of proteins, Biophys. J. 84 (2003) 475–488.
[50] J. Tsai, R. Taylor, C. Chothia, M. Gerstein, The packing density in proteins: standard radii and volumes, J. Mol. Biol. 290 (1999) 253–266.
[51] J.I. Kwiecinska, M. Cieplak, Chirality and protein folding, J. Phys.: Condens. Matter 17 (2005) S1565–S1580.
[52] S.J. Hagen, L. Qiu, S.A. Pabit, Diffusional limits to the speed of protein folding: fact or friction, J. Phys.: Condens. Matter 17 (2005) S1503–S1514.
[53] J. Wang, P. Cieplak, P.A. Kollman, How well does a restrained electrostatic potential (RESP) model perform in calculating conformational energies of organic and biological molecules, J. Comput. Chem. 21,1049 (2000) 1074.
[54] K. Murzyn, M. Pasenkiewicz-Gierula, Construction and optimisation of a computer model for a bacterial membrane, Acta Biochim. Pol. 46 (1999) 631–639.
[55] T. Rog, K. Murzyn, M. Pasenkiewicz-Gierula, The dynamics of water at the phospholipid bilayer surface: a molecular dynamics simulation study, Chem. Phys. Lett. 352 (2002) 323–327.
[56] T. Darden, D. York, L. Pederson, Particle mesh Ewald: an N×log(n) method for Ewald sums in large systems, J. Chem. Phys. 98 (1993) 10089–10092.
[57] E. Orlandini, F. Seno, J.R. Banavar, A. Laio, A. Maritan, Deciphering the folding kinetics of transmembrane helical proteins, Proc. Natl. Acad. Sci. U. S. A. 97 (2000) 14229–14234.
[58] S.B. Fowler, R.B. Best, J.L. Toca Herrera, T.J. Rutherford, A. Steward, E. Paci, M. Karplus, J. Clarke, Mechanical unfolding of a titin Ig domain: structure of unfolding intermediate revealed by combining AFM, molecular dynamics simulations, NMR and protein engineering, J. Mol. Biol. 322 (2002) 841–849.
[59] P.M. Williams, S.B. Fowler, R.B. Best, J.L. Toca-Herrera, K.A. Scott, A. Steward, J. Clarke, Hidden complexity in the mechanical properties of titin, Nature 422 (2003) 446–449.
[60] E. Evans, Probing the relation between force-lifetime- and chemistry in single molecular bonds, Annu. Rev. Biophys. Biomol. Struct. 30 (2001) 105–128.
[61] K.T. Sapra, S. Besir, D. Oesterhelt, D.J. Mueller, Characterizing molecular interactions in different bacteriorhodopsin assemblies by single-molecule force spectroscopy, J. Mol. Biol. 355 (2006) 640–650.